7.2), 20 mM Mg acetate, 150 mM NH_4Cl for 20 min at 37°C and for 20 min on ice. Construction of the A-site complex was as described for the P-site complex except that after addition of gene 32 mRNA, 70S ribosomes were first incubated with 50 pmol of *E. coli* $tRNA_f^{Met}$ for 10 min at 37°C, followed by addition of 150 pmol of 5′-Fe-BABE-ASL, then incubation for 20 min at 37°C and 20 min on ice. Hydroxyl radical strand scission was initiated as described (*17*). Extraction of rRNAs, primer extension, and gel electrophoresis were carried out as described (*43*). All of the observed Fe-BABE–dependent strand scissions were observed in at least three independent experiments and were quantified by PhosphorImager analysis (Molecular Dynamics).

21. S. Joseph and H. F. Noller, unpublished data.
22. S. Arnott, D. W. L. Hukins, S. D. Dover, *Biochem. Biophys. Res. Commun.* **48**, 1392 (1972).
23. S. Sköld, *Nucleic Acids Res.* **11**, 4923 (1983).
24. D. Moazed, J. M. Robertson, H. F. Noller, *Nature* **334**, 362 (1988).
25. The anticodons of two $tRNA^{Phe}$ molecules were base-paired to adjacent codons on a poly(U) mRNA by least-squares fitting to standard A-form helical geometry (*22*). Torsion angles at the junction of the A and P codons were then adjusted until the base-base distances between the A and P tRNAs converged on the values obtained by fluorescence resonance energy transfer (*44*). Independently, they were adjusted to satisfy constraints from hydroxyl-radical probing of A-site tRNA by P-site ASLs, and vice versa (*21*). Both sets of experimental constraints were satisfied well by the arrangement shown in Fig. 6, in which the resulting angle between the planes of the two tRNAs is about 60°. This arrangement is very similar to that originally predicted by Sundaralingam *et al.* (*45*). The structure of ASL33, modeled from the anticodon stem-loop of $tRNA^{Phe}$, extended to 33 bp by standard RNA A helical geometry (*22*), was then docked on each tRNA by least-squares superimposition of ASL4 on nt 28 to 42 of $tRNA^{Phe}$. The predicted locations of the rRNA targets relative to the two tRNAs are independent of the arrangement of the tRNAs; the A- and P-site clouds are, in effect, attached to their respective tRNAs and will simply move along with them.
26. Strong cleavages were defined as those that give rise to gel bands whose intensities are at least two-fold as strong as those of the nearby dideoxy sequencing bands; medium-strength cleavages, as those whose intensities are similar; and weak cleavages, as those whose intensities are half of or less than those of the sequencing bands. Target distances were calibrated in two independent ways. In one case, RNA-RNA duplexes were formed, in which the 5′ end of one strand was derivatized with the Fe(II) probe, and cleavage of the opposite strand was monitored by primer extension. The other approach is an internal calibration inherent in the ASL cleavage data themselves; a lower limit of the probing range for a strong hit at a given target site is half the distance between the two most widely separated ASL tethering sites from which strong cleavage is observed. For example, the maximum separation observed between probe positions for two strong cleavages at the same target is position 1924 by ASL6 and ASL10 (Fig. 3G), corresponding to a distance of about 20 Å between the corresponding ASL phosphate positions. The distance to the target can be estimated as half this distance (10 Å) plus or minus the length of the tether arm (12 Å). This gives a distance range of 0 to 22 Å between the tethering position and target position for strong cleavages. By similar reasoning, we estimate medium-strength cleavages to indicate a range of 12 to 36 Å, and weak cleavages, a range of 20 to 44 Å. The data obtained by means of the duplex method fall into these overlapping ranges, providing independent validation of the values derived from internal calibration. These values are also in good agreement with those reported in previous studies (*27*).
27. G. B. Dreyer and P. B. Dervan, *Proc. Natl. Acad. Sci. U.S.A.* **82**, 968 (1985); H. E. Moser and P. B. Dervan, *Science* **238**, 645 (1987); T. D. Tullius, *Free Radic. Res. Commun.* **2**, 521 (1991); H. Han and P. B. Dervan, *Proc. Natl. Acad. Sci. U.S.A.* **91**, 4955 (1994).
28. P. Gornicki, K. Nurse, W. Hellmann, M. Boublik, J. Ofengand, *J. Biol. Chem.* **259**, 10493 (1984); T. Wagenknecht, J. Frank, M. Boublik, K. Nurse, J. Ofengand, *J. Mol. Biol.* **203**, 753 (1988).
29. S. Stern, B. Weiser, H. F. Noller, *J. Mol. Biol.* **204**, 447 (1988); R. Brimacombe, J. Atmadja, W. Stiege, D. Schuler, *ibid.* **199**, 115 (1988).
30. D. L. Fink, R. O. Chen, H. F. Noller, R. B. Altman, *RNA* **2**, 851 (1996).
31. H. Stark *et al.*, *Cell* **88**, 19 (1997).
32. M. Santer *et al.*, *Proc. Natl. Acad. Sci. U.S.A.* **87**, 3700 (1990); W. E. Tapprich, D. J. Goss, A. E. Dahlberg, *ibid.* **86**, 4927 (1989).
33. J. Frank *et al.*, *Nature* **376**, 441 (1995).
34. H. Stark *et al.*, *Structure* **3**, 815 (1995).
35. H. F. Noller, *Annu. Rev. Biochem.* **60**, 191 (1991); R. Green and H. F. Noller, *ibid.* **66**, 679 (1997).
36. I. Leviev, S. Levieva, R. A. Garrett, *Nucleic Acids Res.* **23**, 1512 (1995).
37. J. Thompson, F. Schmidt, E. Cundliffe, *J. Biol. Chem.* **257**, 7915 (1982).
38. D. Moazed and H. F. Noller, *Biochimie* **69**, 879 (1987).
39. M. Oßwald, B. Greuer, R. Brimacombe, *Nucleic Acids Res.* **18**, 6755 (1990).
40. A. Hüttenhofer and H. F. Noller, *Proc. Natl. Acad. Sci. U.S.A.* **89**, 7851 (1992).
41. V. Biou, A. Yaremchuk, M. Tukalo, S. Cusack, *Science* **263**, 1404 (1994).
42. S. V. Kirillov, V. I. Makhno, Y. P. Semenkov, *Nucleic Acids Res.* **8**, 183 (1980).
43. S. Stern, D. Moazed, H. F. Noller, *Methods Enzymol.* **164**, 481 (1988).
44. A. E. Johnson, H. J. Adkins, E. A. Matthews, C. R. Cantor, *J. Mol. Biol.* **156**, 113 (1982); H. Paulsen, J. M. Robertson, W. Wintermeyer, *ibid.* **167**, 411 (1983).
45. M. Sundaralingam, T. Brennan, N. Yathindra, T. Ichikawa, in *Structure and Conformation of Nucleic Acids and Protein–Nucleic Acid Interactions*, M. Sundaralingam and S. T. Rao, Eds. (University Park, Baltimore, MD, 1975), pp. 101–115.
46. We thank C. R. Woese for suggesting the internal calibration strategy; D. P. Greiner, J. Moran, and C. F. Meares for helping with synthesis of BABE and for providing samples of BABE used in early experiments; members of the Puglisi lab for providing T7 RNA polymerase; M. I. Recht for help with EXCEL; K. Lieberman and R. Green for discussions; and J. Cate, G. Culver, L. Newcomb, R. Green, K. Wilson, K. Lieberman, and L. Holmberg for review of the manuscript. Supported by grant GM-17129 from the NIH and from a grant to the Center for Molecular Biology of RNA from the Lucille P. Markey Charitable Trust.

19 March 1997; accepted 19 September 1997

Age and Origin of the Moon

Der-Chuen Lee,* Alex N. Halliday, Gregory A. Snyder, Lawrence A. Taylor

The age and origin of the moon have been studied with the use of the recently developed short-lived hafnium-tungsten chronometer (^{182}Hf-^{182}W, half-life of nine million years). The tungsten isotopic compositions of 21 lunar samples range from chondritic to slightly radiogenic ($\varepsilon_W = -0.50 \pm 0.60$ to $+6.75 \pm 0.42$). This heterogeneity may have been inherited from material excavated from Earth and the putative impactor, but it is more likely the result of late radioactive decay within the moon itself; in this case, the moon formed 4.52 to 4.50 billion years ago, and its mantle has since remained poorly mixed.

The most widely accepted model for the origin of the moon is that during the later stages of Earth's accretion the impact of a colliding planet at least the size of Mars generated both the hot debris to form the moon and the angular momentum of the Earth-moon system (*1*, *2*). Yet, inconsistencies in this model persist (*3*, *4*). For example, it has long been argued on geochemical grounds that most of the material that formed the iron-depleted moon was derived from the silicate Earth after the formation of its core (*4*). This view is disputed by some (*5*), and others have argued, on the basis of their simulations, that the moon must have been derived largely from the mantle of the impactor (*2*, *6*). This latter view is considered by some to be inconsistent with the moon's many "Earth-like" features (*7*, *8*).

The ^{182}Hf-^{182}W [half-life = nine million years (m.y.)] chronometer can be used to investigate this problem. Because hafnium and tungsten are both highly refractory, planets and planetesimals that formed early in the history of the solar system should have relative proportions of these elements similar to those found in chondrites (*9*–*11*). However, Hf is lithophile (silicate-loving), whereas W is normally siderophile (metal-loving), such that core formation results in a dramatic intraplanetary fractionation of Hf and W. If this fractionation takes place during the lifetime of ^{182}Hf, the silicate reservoir, which has a high Hf/W ratio, will develop an excess abundance of ^{182}W relative to that found in chondritic bodies. Impacts

D.-C. Lee and A. N. Halliday are in the Department of Geological Sciences, University of Michigan, Ann Arbor, MI 48109–1063, USA. G. A. Snyder and L. A. Taylor are with the Planetary Geosciences Institute, Department of Geological Sciences, University of Tennessee, Knoxville, TN 37996, USA.

*To whom correspondence should be addressed. E-mail: dclee@umich.edu

Table 1. Hf and W isotopic data. The ε_W of each W isotopic measurement is expressed as the deviations in parts per 10^4 relative to the NIST-3163 W standard, which gives a $^{182}W/^{184}W = 0.865000 \pm 18$ ($n = 20$). For all samples, T_{CHUR} is calculated assuming $(^{180}Hf/^{184}W)_{chond} = 1.568 \pm 0.078$, $(^{182}W/^{184}W)_{chond} = 0.864985 \pm 25$, and a $^{180}Hf/^{184}W = 55 \pm 35$ for the lunar magma ocean, with the exception of the A-17 picritic orange glasses, for which we used the measured $^{180}Hf/^{184}W$. Concentrations are in parts per million or billion (ppm and ppb). SE, standard error; Qz, quartz; Ol, olivine; norm., normative.

Sample		Hf (ppm)	W (ppb)	$^{180}Hf/^{184}W$	$^{182}W/^{184}W$ $\pm 2\sigma$ SE	$\varepsilon_W \pm 2\sigma$ SE	T_{CHUR} (m.y. $\pm 2\sigma$)
Type	Number						
				Terrestrial			
Loihi	1802-4A	2.804	148.6	22.26	0.864992 ± 33	−0.09 ± 0.38	—
Atlantic MORB	A127 (D-15)	1.227	100.7	14.37	0.865021 ± 31	+0.24 ± 0.36	—
				Mare basalts			
High-Al basalt	14053	6.766	326.2	24.47	0.864993 ± 42	−0.08 ± 0.48	—
Picritic basalt	15385	1.369	69.7	23.2	0.86504 ± 13	+0.4 ± 1.5	—
Qz-norm. basalt	15475	2.15	59.0	43.2	0.864953 ± 52	−0.50 ± 0.60	—
Ol-norm. basalt	15016-1	2.597	137	22.3	0.865382 ± 83	+4.4 ± 0.96	45^{+7}_{-17}
Ol-norm. basalt	15016-2	2.573	114	26.6	0.865331 ± 78	+3.8 ± 0.82	47^{+7}_{-18}
Ol-norm. basalt	15555	2.16	77.0	32.8	0.865584 ± 36	+6.75 ± 0.42	40^{+7}_{-16}
High-Ti basalt	10032	16.79	428.8	46.20	0.865205 ± 43	+2.37 ± 0.50	53^{+7}_{-17}
Pigeonite basalt	12011	3.680	148.7	29.19	0.865115 ± 54	+1.33 ± 0.62	60^{+8}_{-24}
Ilmenite basalt	12045	4.162	92.0	53.4	0.865416 ± 83	+4.81 ± 0.96	44^{+7}_{-17}
Lunar meteorite	Asuka-881757	2.812	73.70	45.04	0.865102 ± 71	+1.18 ± 0.82	61^{+9}_{-18}
				KREEP basalts			
	15382	22.86	1223	22.05	0.865133 ± 26	+1.54 ± 0.30	58^{+7}_{-18}
	15386	30.51	1743	20.66	0.865193 ± 22	+2.23 ± 0.26	53^{+7}_{-17}
				Apollo 17 soils			
Picritic orange glass	74220 (bulk)	5.807	226.4	30.27	0.865086 ± 55	+0.99 ± 0.64	55^{+7}_{-14}
Picritic orange glass	74220 (picked)	4.852	68.6	83.5	0.86544 ± 12	+5.0 ± 1.4	49^{+4}_{-6}
Picritic orange glass	74241 (bulk)	6.969	208.0	39.54	0.865235 ± 71	+2.72 ± 0.82	47^{+4}_{-7}
				Highlands			
Ferroan anorthosite	60025	0.0282	4.03	8.27	0.86526 ± 14	+3.1 ± 1.7	50^{+8}_{-27}
Ferroan anorthosite	65315	0.00403	6.48	0.734	0.865156 ± 93	+1.8 ± 1.1	56^{+8}_{-30}
Ferroan anorthosite	15415	0.0134	7.26	2.18	0.86500 ± 12	0.0 ± 1.4	—
Ferroan anorthosite	62255	0.0239	3.46	8.15	0.86499 ± 21	−0.07 ± 2.4	—
Troctolite	76535	0.2699	28.46	11.19	0.865266 ± 55	+3.08 ± 0.64	50^{+7}_{-17}
Norite	78235	1.085	568.9	2.251	0.865063 ± 14	+0.73 ± 0.16	66^{+8}_{-20}
Norite	77215	3.213	276.6	13.71	0.865060 ± 14	+0.69 ± 0.16	67^{+8}_{-21}
Mg-granulite	67955	1.948	157.0	14.65	0.865039 ± 29	+0.40 ± 0.34	—

after the core has formed can result in entire planetary bodies, such as the moon, with nonchondritic lithophile- to siderophile-element (hence Hf/W) ratios. The W isotopic composition of the moon would be expected largely to reflect that inherited from the particular mixture of silicate-rich debris derived from Earth, and the impactor at the time the moon formed (*9*, *10*). However, it is also possible that W isotopic heterogeneity was generated within the moon itself as a result of the decay of live ^{182}Hf. Radioactive decay is an exponential process, such that sufficiently large parent-to-daughter (Hf/W) ratios can still produce observable W isotopic variations at a late stage. It is thought that the earliest history of the moon may have involved a magma ocean, which could have fractionated Hf/W to such extreme values (*11*).

The geology of the moon. Despite its small size, the moon had an active igneous history that lasted throughout its first 1.5 billion years, resulting in a differentiated crust and probably a small Fe-rich core (*5*, *12*). The most prominent igneous rocks on the lunar surface, constituting over 90% of the crust, are ferroan anorthosites and Mg-rich rocks (in roughly equal proportions) from the lunar highlands. Mare basalts cover about 17% of the lunar surface but constitute only ~1% of the crust (*12*, *13*). Other rock types such as KREEP basalt (enriched in the incompatible trace elements, potassium, the rare earths, and phosphorous), picritic volcanic glass, dunite, alkali anorthosite, and granite have been reported, but are much less abundant (*12*).

Some of the lunar highlands rocks appear to be very old [>4.4 billion years (Ga)] and may relate to the earliest magmatic conditions that immediately followed the giant impact (*14*–*19*). Because of its global distribution and uniform molar Ca/(Ca + Na) ratio of ~0.96, some ferroan anorthosites are considered to have formed by the flotation of light plagioclase on top of dense basaltic magmas, possibly on a global scale (*12*, *20*, *21*). Others, however, are too young to be of the same origin (*22*). Many Mg-rich rocks exhibit evidence of being intrusive cumulates; others are considered products of impact-induced melting (*12*, *23*).

All mare basalts are ≤4.2 Ga in age and are compositionally diverse. Judging by their liquidus phases, they could have been derived from a range of depths (*24*). The prominent negative Eu anomalies in mare basalts are thought to be caused by the melting of ultramafic cumulates that were precipitated during the extraction of anorthositic crust in a magma ocean (*12*, *24*). The liquid residuum of this putative magma ocean should have been enriched in incompatible trace elements and may be a source of KREEP basalts (*12*, *23*). Finally, the lunar volcanic glasses represent picritic melts erupted by fire fountaining, and derived from great depth (200 to 1000 km) below the mantle that formed in the magma ocean (*7*, *24*, *25*).

Tungsten isotopic heterogeneity in the moon. We have analyzed a broad range of the above rock types (*26*) and a lunar meteorite found in Antarctica, Asuka 881757, considered to be a mare basalt (*27*) (Table 1). All of the lunar samples yielded W isotopic compositions (*28*) that are, within uncertainty, chondritic (*29*) or radiogenic (*30*) (Table 1). The only previous W isotopic measurement for a lunar sample was on mare basalt 14053 (9), which was chondritic within uncertainty. A repeat measurement of this sample yielded a consistent but more precisely defined isotopic composition (*31*) of $\varepsilon_W = -0.08 \pm 0.48$. However, only two other mare basalts, two ferroan anorthosites, and the Mg-granulite yielded W isotopic compositions that are chondritic within uncertainty; the rest all have a resolvable ^{182}W excess (ε_W = +0.7 to +6.75) (Fig. 1).

All of the highlands samples included in this study, with the exception of the Mg-granulite (67955), are old and pristine (*26*). Therefore, it is unlikely that the W isotopic compositions have been affected by contamination. This assumption is endorsed by the fact that the anorthosites define a range of W isotopic compositions ($\varepsilon_W = -0.07 \pm 2.4$ to $+3.1 \pm 1.7$) identical to that of the Mg-suite rocks ($\varepsilon_W = +0.40 \pm 0.34$ to $+3.1 \pm 0.6$), despite more than an order of magnitude difference in W concentration. No correlation exists between Hf/W ratio and W isotopic compositions among the eight highlands samples, such as might be expected if the isotopic variations reflected in situ decay (Table 1 and Fig. 2A). This decoupling is most convincingly shown by the two A-17 norites, which have Hf/W ratios that differ by a factor of 6 but have identical W isotopic compositions. The two highlands samples with the most radiogenic W (ε_W = +3), anorthosite 60025 and troctolite 76535, yielded very old ages when measured by long-lived chronometers, although the exact age of the troctolite is debated (*26*). These samples would need to have formed within the first 30 m.y. of solar system history for these W isotopic excesses to reflect in situ decay. This history is improbable because U-Pb and Sm-Nd ages for these samples are all <4.53 Ga (*26*). The W isotopic variations are more likely inherited from their parent magmas and were present during the earliest stages of the moon's development.

The mare basalts, including lunar meteorite Asuka 881757, define a range of W isotopic compositions ($\varepsilon_W = -0.50 \pm 0.60$ to $+6.75 \pm 0.42$) that completely overlaps those of the highland rocks, the KREEP basalts ($+1.54 \pm 0.30$ and $+2.23 \pm 0.26$), and the Apollo 17 orange soils ($+0.99 \pm 0.64$ to $+5.0 \pm 1.4$) (Table 1 and Fig. 1). As with the highland rocks, no correlation exists between Hf/W ratio and W isotopic compositions among the mare basalts (Fig. 2A), which is consistent with the derivation of these relatively young magmas from source regions that may have had a complex petrogenetic history. The W isotopic variations must have been generated by radioactive decay within the first 100 m.y. of the

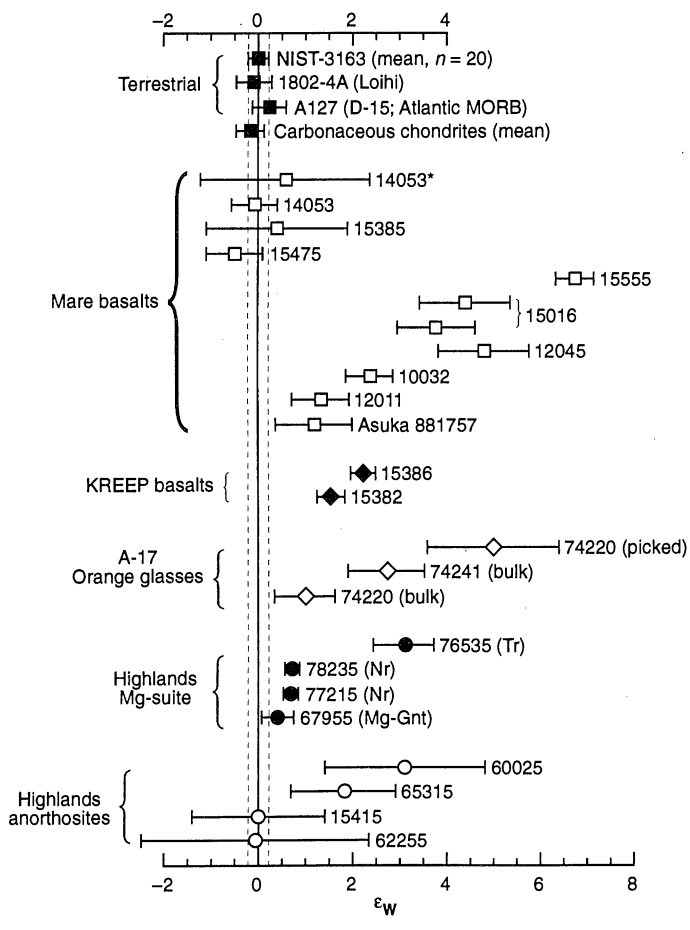

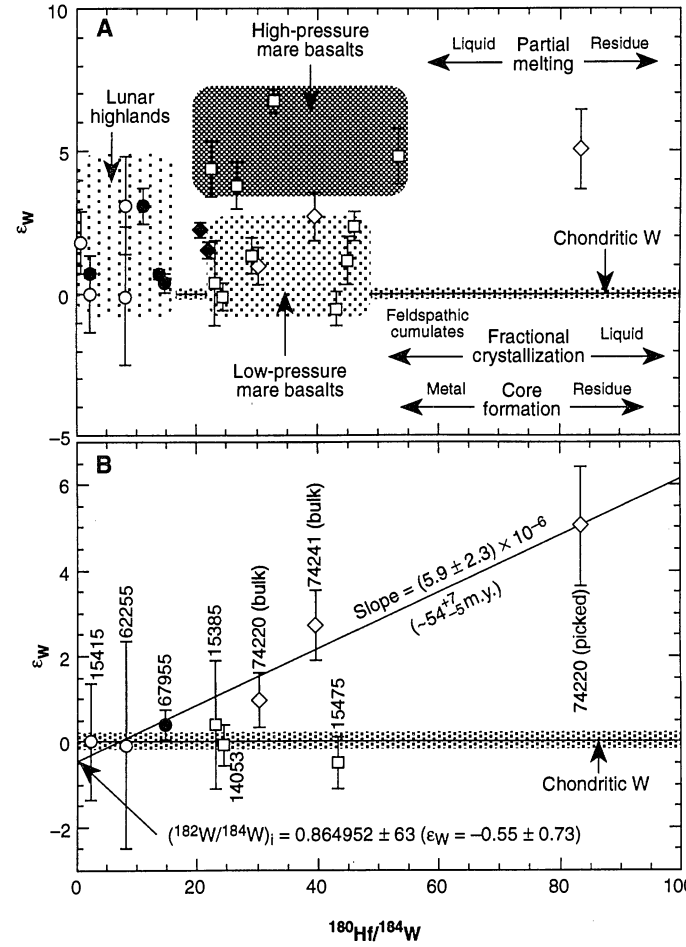

Fig. 1. (**Left**) The ε_W values of samples analyzed in this study (Table 1). Also plotted are previously reported data, including the mean of carbonaceous chondrites (*29*) and mare basalt 14053 (*9*) (shown with an asterisk). **Fig. 2.** (**Right**) (**A**) $^{180}Hf/^{184}W$ versus ε_W for all the lunar samples analyzed in this study (Table 1). Symbols are the same as in Fig. 1. (**B**) $^{180}Hf/^{184}W$ versus $^{182}W/^{184}W$ for A-17 orange glasses and lunar samples with chondritic W isotopic compositions. The best-fit line is based on the data for the three A-17 orange glasses only.

solar system, whereas the basalts are all ≤4.2 Ga in age. Even if the variations developed by decay within the moon itself, the intervening history of remelting would be expected to modify the Hf/W ratios in the lunar mantle on a small scale. A similar decoupling of W isotopic composition from Hf/W has been found in martian meteorites (*30*), again reflecting the relatively young formation age for the samples.

Phase relations are consistent with a deep (higher pressure) source for the olivine-normative basalts 15016 and 15555 and the ilmenite basalt 12045 (*24*). These samples are characterized by very radiogenic W ($\varepsilon_W \geq +4$), notably 15555. Conversely, 12011, 15385, and 15475, with chondritic W isotopic compositions, have low-pressure–phase assemblages (*24*). High-Ti basalts such as 10032 cover a broad range of assemblages. The simplest explanation for this mix is that the lunar mantle is stratified isotopically, with a more radiogenic W isotopic composition toward its deep interior. This heterogeneity has probably survived since the earliest history of the moon and provides powerful evidence against large-scale convective mixing of the lunar mantle. Data for the A-17 orange glasses are consistent with this finding because they are considered to have been derived from depth greater than the mare basalts (*25*). The bulk samples are largely glass but contain a mixture of components, some extremely fine grained. Hand-picked and cleaned coarser glass beads from 74220 yield particularly radiogenic W ($\varepsilon_W = +5.0 \pm 1.4$).

Accretionary origin for lunar W isotope heterogeneity. Two classes of models explain the above results: Either the variations were inherited as heterogeneities from Earth and the moon-forming impactor, or the moon differentiated sufficiently early that radiogenic W was generated by decay within the moon itself. The latter appears more likely. Whichever is correct, the isotopic variations could only have been produced within the first 100 m.y. of the solar system, long before the melting that produced the mare basalts. Although any viable model has to explain the apparent relation between the depth of melting and W isotopic composition of these basalts, thereby reflecting in some way the large-scale internal structure of the moon, neither model predicts any particular relation between W isotopic composition and the Hf/W of the samples because the source regions and magmas themselves may have experienced considerable subsequent fractionation of Hf/W.

Because W is highly incompatible, most of the silicate Earth's inventory resides in the continental crust (*11*). Sample NIST-3163, representative of the crustal W isotopic composition, is chondritic to within 0.5 ε_W units. We have checked for W isotopic heterogeneity in the silicate Earth by analyzing an andesite standard (AGV-1), a continental tholeiite standard (WS-E), an Atlantic mid-ocean ridge basalt (MORB) glass (A127), and a Loihi OIB glass (1802-4A). All of these are chondritic (Table 1) (*9*, *29*). If the moon were derived from the silicate Earth today, it would have chondritic W, whereas the compositions of lunar samples are chondritic or radiogenic.

The isotopic variations could reflect incomplete mixing of debris from Earth and the impactor. It is also possible that the current state of the silicate Earth does not accurately reflect the conditions at the time the moon formed. Tungsten isotopic heterogeneity is expected in a growing planet undergoing concomitant core formation, and the average composition of the silicate Earth could have been radiogenic when the moon formed but chondritic today (*10*). Similarly, there is nothing in the W isotope data to preclude the possibility that the heterogeneity was inherited from the impactor (*30*). There are, nevertheless, reasons for doubting any of these explanations, given current thinking about the composition and origin of the moon.

The reason why a small, late, K-depleted body such as the moon developed a magma ocean at all is almost certainly the phenomenal accretional energy associated with its birth. Dynamic simulations of the impact involve temperatures of >10,000 K and the redistribution of matter on a planetary scale (*2*). It is inconceivable that W isotope heterogeneity survived this process, let alone preserved as a stratified feature of the lunar mantle. The moon would instead have to form in stages from distinct parent bodies. Recent simulations sometimes generate multiple fragments that eventually collide to form the present moon (*6*). However, these fragments are derived from the same source, and the final collision is unlikely to preserve an isotopically layered moon.

Late addition of a chondritic veneer (*32*) might generate heterogeneities by variably diluting radiogenic W. However, the W isotope heterogeneity has been a part of the moon since its earliest history, whereas the veneer was probably added up until 3.9 Ga (*10*). Finally, W/U and Ba/Rb ratios in basalts formed by remelting of the differentiated lunar mantle are uniform and nonchondritic, implying that the mantle was well-mixed at one stage (*4*, *5*). Inherited W isotopic heterogeneity is difficult to explain in a manner consistent with this observation.

Early lunar differentiation and W isotope heterogeneity. In contrast to the above "inheritance" models, the generation of W isotopic heterogeneity by ^{182}Hf decay during lunar differentiation and core formation is fully consistent with current models and data for the moon. The moon inherited a high Hf/W ratio (~20), but early lunar core formation and extraction of low-Hf/W silicate melts, leading to a low-Hf/W crust, must have left a depleted residual mantle with Hf/W ratios higher than that of the bulk moon. If the moon formed sufficiently early, these reservoirs would generate relatively radiogenic W, whereas those with lower Hf/W would retain chondritic W. The W isotopic variations in the mare basalts, therefore, reflect remelting of heterogeneities produced by radioactive decay within the magma ocean, ultramafic cumulate pile, and residual mantle. Protracted remelting and mixing at shallow depths may have eventually partially rehomogenized the W isotopic composition of the crust and uppermost mantle such that low-pressure mare basalts were erupted from reservoirs with approximately chondritic W isotopic compositions.

The basaltic samples analyzed span an age range of 4.1 to 3.2 Ga (*33*), covering almost the entire history of mare magmatism. Although some of the highlands samples could have formed extremely early and sampled W isotopic variability that was subsequently homogenized, the preservation of W isotopic variations in the source regions of the basalts requires negligible mixing of the lunar interior since its earliest differentiation. The magma ocean is thought by some to have persisted until 4.4 Ga (*12*), long after ^{182}Hf would have become extinct. It is difficult to reconcile the W data with models that involve a long-lived (≥200 m.y.), globally extensive, largely molten magma ocean (*12*) undergoing major convective overturn (*34*), because this process will effectively erase any W isotopic anomalies. Therefore, any magma ocean must have rapidly become partially restricted and unable to mix in order to limit homogenization of the W isotopic variations to the shallowest portions. A partially molten magma ocean (*20*) is less likely to have reached global W isotopic equilibrium.

The age and origin of the moon. The orange glasses display a correlation between W isotopic composition and Hf/W ratios that is consistent with the preservation of a relation between the W isotopic compositions and the parent/daughter ratios in their source regions (Fig. 2B). Strictly speaking, this relation must be a mixing line, and the time significance of

the slope depends on the relations among the components in the soil. However, it is considered most likely that these various components were derived as melts from the interior of the moon. These particular soil samples are extremely rich in volcanic glass and meteoritic contamination is negligible (*25*). This composition is confirmed by the fact that the bulk samples contain even higher Hf concentrations than the hand-picked glass (Table 1). This result would be consistent with dilution by other lunar melts such as KREEP basalts (Table 1) forming part of the finer grained material, but is difficult to reconcile with any kind of meteoritic contamination.

The Hf/W and W isotopic heterogeneity in the orange glasses most likely reflects "scavenging" of melt from the mantle at great, but variable, depth (*25*). Given that the glasses are picritic and represent large degrees of partial melting, it is quite likely that the Hf/W ratios were not fractionated by melting, and the slope of the apparent isochron (Fig. 2B) may define the timing of the formation of this W isotope heterogeneity. The isochron age obtained from the orange glass data is 54^{+7}_{-5} m.y. (2σ). The intercept is chondritic within uncertainty, as expected if the isochron defines the time of differentiation from a parent body with chondritic time-integrated Hf/W.

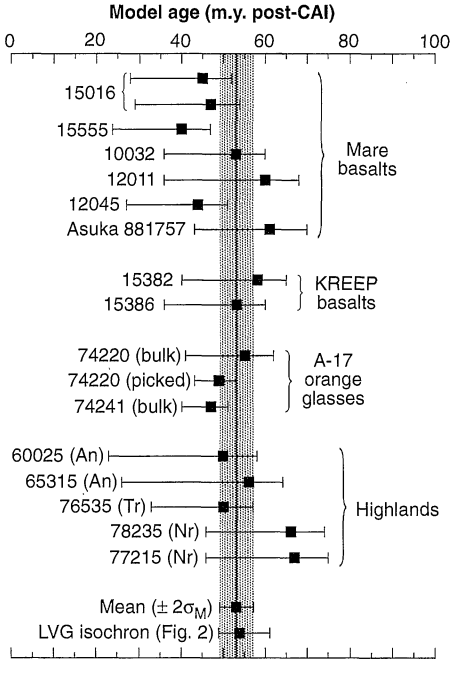

Fig. 3. T_{CHUR} (in millions of years, $\pm 2\sigma$) for lunar samples with nonchondritic W isotopic compositions (Table 1) (*39*). The mean of all the model ages, 53 ± 4 m.y. ($\pm 2\sigma_M$), and the isochron age for the A-17 lunar volcanic glasses (LVG) from Fig. 2B are also shown for comparison.

With the possible exception of the Apollo 17 orange glasses, there is no evidence that any of the W isotopic compositions are directly related to the measured parent/daughter ratios. Although this lack of evidence is entirely reasonable given the history of the moon, it means that the determination of isotopic ages has to be based on certain model assumptions. In particular, it is necessary to use a reliable estimate of the maximum range in parent/daughter ratios that could have generated the isotopic compositions and to incorporate this variability directly into the calculation of the age uncertainty. Fortunately, isotopic variations produced by short-lived decay provide relatively accurate age constraints on early solar system chronologies, even if the parent/daughter ratios have large uncertainties. Using the Hf-W system, we can determine an age for the moon that is inherently more accurate and reliable than those obtained with the use of any long-lived decay system, simply because the window of time for producing variations, such as those reported here, is extremely narrow.

The mean $^{180}Hf/^{184}W$ atomic ratio (= 1.18 × Hf/W weight ratio) for all lunar basalts in Table 1 is 36 ± 17 (1σ). This variability is comparable to that of highly incompatible element ratios such as Ba/Nb and Ce/U ratios in terrestrial MORBs (*35*) and implies that there has been only moderate fractionation from source ratios during melting. Indeed, the highly enriched KREEP basalts have Hf/W ratios that are only slightly lower than the mare basalts and picritic orange glasses (Table 1). The behavior of W during melting on the moon appears to have been different from its behavior on Earth. In terrestrial basalts, W is highly incompatible with a bulk distribution coefficient D comparable to that of Ba, Rb, or Ra (*36*). Hafnium, in contrast, is only moderately incompatible in terrestrial mantle melting, leading to two orders of magnitude variability in Hf/W in modern oceanic basalts (*36*). The obvious explanation for this difference between Earth and the moon is that W was much less incompatible during lunar mantle melting, with a bulk D only slightly less than, or similar to, that for Hf. Similar behavior has also been noted for Re (*37*) and In (*38*). This difference is probably because mare basalts are so highly reduced that they formed at or near iron metal saturation (*24*).

In estimating the Hf/W ratio of the lunar magma ocean that generated the W isotopic compositions, we took a conservative approach. The lowest Hf/W ratios of the lunar basalts are those of the KREEP samples (Table 1), and it is reasonable to assume that the magma ocean had a higher value ($^{180}Hf/^{184}W > 20$). The highest $^{180}Hf/^{184}W$ measured is for the separated orange glass (Table 1); given that this sample is an extreme composition from a picritic liquid at great depth, it is reasonable to assume that the magma ocean had a $^{180}Hf/^{184}W < 90$. Therefore, to avoid a sampling bias, we used $^{180}Hf/^{184}W = 55 \pm 35$, which covers this entire range for the basaltic samples (Table 1; mean = 36 ± 17). The Hf/W ratio of the magma ocean from which the highlands cumulates precipitated was probably slightly lower, but this difference has little effect on the age calculation. A Hf-W model age T_{CHUR} (*30*, *39*) can then be calculated for the average protolith material of both the highlands rocks and the basalts. These model ages (Table 1 and Fig. 3) represent the model time after the start of the solar system when Hf/W ratios were fractionated as a result of differentiation from a chondritic reservoir (*30*, *39*). The late addition of material with chondritic Hf/W and W isotopic composition, such as a late veneer, has negligible effect on the ages.

The average model age for the mare basalts calculated in this fashion is 50 ± 16 m.y. (2σ). Using the measured Hf/W ratios of the mare basalts instead of the model mantle value yields a similar average model age of 44 ± 19 m.y. Because the orange glasses are thought to be large-degree partial melts of a source deeper than the crystalline magma ocean, we instead used the measured Hf/W ratios to calculate model ages for their sources. The mean T_{CHUR} for the KREEP basalts (56 ± 7 m.y.), the A-17 orange glasses (50 ± 8 m.y.), and the highlands rocks (58 ± 17 m.y.) overlap the mare basalt mantle model ages. There is no reason why all of these rocks, which sample the moon as magmas from the surface to its deep interior over a time span of 1.5 billion years, should give about the same result unless this period defines the time of major lunar differentiation, probably associated with the earliest history of the moon. This age is also implied by the orange glass data, which define an apparent isochron age of 54^{+7}_{-5} m.y. (2σ), with chondritic initial W isotopic composition (Fig. 2B), in excellent agreement with the mean model age of all lunar samples at 53 ± 4 m.y. ($2\sigma_M$) (Fig. 3). The consistency between Hf-W model ages and the isochron age (Fig. 3) suggests that the best-fit line in Fig. 2B provides meaningful age information and that all of these ages define the timing of a global lunar differentiation, including the formation of a magma ocean. On the basis of these data, we estimate that the moon formed and differentiated ~50 m.y.

after the start of the solar system, within the time window 4.52 to 4.50 Ga. This time corresponds to the earliest of previous estimates (*10*, *14*–*19*, *33*).

It is unlikely that terrestrial core formation occurred after the giant impact that formed the moon. The chondritic W isotopic composition of the silicate Earth also places an upper limit of 4.515 Ga on the timing of terrestrial core formation, unless terrestrial accretion was slow (*10*). The initial W isotopic composition of the lunar volcanic glasses source at ~4.51 Ga, as defined by the intercept on Fig. 2B, is, within error, identical to chondritic W, indicating that the protolith had a chondritic Hf/W for most of its history, consistent with the chondritic W isotopic compositions of some of the lunar samples and the chondritic first stage implicit in the Hf-W model ages. Recent Hf-W studies of eucrites, iron meteorites, and martian meteorites suggest that differentiation between metal and silicate (or core formation) occurred early (within 10 m.y.) in their respective parent bodies (*9*, *29*, *30*). If the moon originated primarily from the silicate portion of a planet that differentiated early, it is expected to have left a similar radiogenic W isotopic signature throughout the entire moon. The chondritic initial W isotopic composition of the moon is, therefore, consistent with the hypothesis that the moon was derived from Earth, or an impactor with a history of accretion and metal segregation similar to that found in Earth (*4*–*8*).

REFERENCES AND NOTES

1. W. K. Hartman, in *Origin of the Moon*, W. K. Hartman, R. J. Phillips, G. J. Taylor, Eds. (Lunar Planetary Institute, Houston, TX, 1986), pp. 579–608; D. J. Stevenson, *Annu. Rev. Earth Planet. Sci.* **15**, 271 (1987).
2. H. J. Melosh, in *Origin of the Earth*, H. E. Newsom and J. H. Jones, Eds. (Oxford Univ. Press, Oxford, 1989), pp. 69–83; A. G. W. Cameron and W. Benz, *Icarus* **92**, 204 (1991).
3. A. E. Ringwood, Ed., in *Origin of the Earth and the Moon* (Springer-Verlag, New York, 1979).
4. W. Rammensee and H. Wänke, *Proc. Lunar Planet. Sci. Conf.* **8**, 399 (1977); H. Wänke and G. Dreibus, in *Origin of the Moon*, W. K. Hartman, R. J. Phillips, G. J. Taylor, Eds. (Lunar Planetary Institute, Houston, 1986), pp. 649–672; H. E. Newsom, *ibid.*, pp. 203–229.
5. H. E. Newsom and M. J. Drake, *Nature* **297**, 210 (1982); H. E. Newsom and S. R. Taylor, *ibid.* **338**, 29 (1989); J. H. Jones and M. J. Drake, *Geochim. Cosmochim. Acta* **57**, 3785 (1993); S. R. Taylor and T. M. Esat, in *Earth Processes: Reading the Isotopic Code*, A. Basu and S. Hart, Eds. (American Geophysical Union, Washington, DC, 1996), pp. 33–46.
6. A. G. W. Cameron, *Lunar Planet. Sci.* **XXVII**, 988 (1997); S. Ida, R. M. Canup, G. P. Stewart, *Nature* **389**, 353 (1997).
7. A. E. Ringwood, *Earth Planet. Sci. Lett.* **111**, 537 (1992).
8. R. N. Clayton and T. Mayeda, *Proc. Lunar Planet. Sci. Conf.* **6**, 1761 (1975); A. E. Ringwood, *Earth Planet. Sci. Lett.* **95**, 208 (1989).
9. D.-C. Lee and A. N. Halliday, *Nature* **378**, 771 (1995).
10. A. N. Halliday, M. Rehkämper, D.-C. Lee, W. Yi, *Earth Planet. Sci. Lett.* **142**, 75 (1996).
11. H. E. Newsom *et al.*, *Geochim. Cosmochim. Acta* **60**, 1155 (1996).
12. P. H. Warren, *Annu. Rev. Earth Planet. Sci.* **13**, 201 (1985).
13. C. R. Neal and L. A. Taylor, *Geochim. Cosmochim. Acta* **56**, 2177 (1992).
14. G. W. Lugmair, K. Marti, J. P. Kurtz, N. B. Scheinin, *Proc. Lunar Planet. Sci. Conf.* **7**, 2009 (1976).
15. N. Nakamura *et al.*, *ibid.*, p. 2309.
16. D. A. Papanastassiou and G. J. Wasserburg, *ibid.*, p. 2035.
17. B. B. Hanan and G. R. Tilton, *Earth Planet. Sci. Lett.* **84**, 15 (1987).
18. R. W. Carlson and G. W. Lugmair, *ibid.* **90**, 119 (1988).
19. W. R. Premo and M. Tatsumoto, *Lunar Planet. Sci.* **XXI**, 89 (1991).
20. D. N. Shirley, *J. Geophys. Res.* **88**, 519 (1983).
21. G. A. Snyder, L. A. Taylor, C. R. Neal, *Geochim. Cosmochim. Acta* **56**, 3809 (1992).
22. L. Borg *et al.*, *Meteoritics Planet. Sci.* **32** (suppl. A), 18 (1997).
23. G. A. Snyder, C. R. Neal, L. A. Taylor, A. N. Halliday, *J. Geophys. Res.* **100**, 9365 (1995).
24. J. Longhi, *Geochim. Cosmochim. Acta* **56**, 2235 (1992); D. Walker, J. Longhi, E. M. Stolper, T. L. Grove, J. F. Hayes, *ibid.* **39**, 1219 (1975).
25. J. C. Meyer, D. S. Mckay, D. H. Anderson, P. Butler Jr., *Proc. Lunar Planet. Sci. Conf.* **6**, 1673 (1975); J. W. Delano, *J. Geophys. Res.* **91**, 201 (1986).
26. Highlands rocks display a large spread in Hf and W concentrations, consistent with their variable cumulate mineralogy, the anorthosites being the most depleted (Table 1). Intense meteorite bombardment may result in brecciation and variable contamination of these samples (*23*). This alteration is a particular problem for the ferroan anorthosites, which have only a few parts per billion of W (Table 1). Average solar system debris is probably chondritic in terms of W isotopic composition, but the average may not be relevant to a particular sample. To minimize this problem, we selected samples with a high confidence class (cc) (*40*), which is an index of pristinity, with 9 being the most pristine. All four ferroan anorthosites studied have cc ≥ 8. Where possible, we have also used samples with reasonably well-preserved Sm-Nd and U-Pb systematics. Most ferroan anorthosites are thought to be early, but sample 60025 (*41*) is particularly important in this respect: With a Sm-Nd age of 4.44 ± 0.02 Ga (*18*) and a Pb-Pb age of 4.51 ± 0.01 Ga (*17*), it has the most reliable age of any early lunar rock. Although troctolite 76535 (cc = 9) yields a Rb-Sr age of 4.61 ± 0.07 Ga (*16*), some have argued that the Sm-Nd age of 4.26 ± 0.06 Ga (*14*) may be closer to the correct value. For the norites, we used 77215 (cc = 8), which yields a Sm-Nd age of 4.37 ± 0.07 Ga (*15*), and 78235 (cc = 8), with a Pb-Pb age of 4.43 ± 0.07 Ga (*19*); both of these norites have exceedingly high W concentrations (Table 1). The Mg-granulite 67955 is a cataclasized poikiloblastic noritic anorthosite; of all of the samples, it is the least pristine and the most likely to be contaminated with meteoritic siderophiles. Its exact age is unclear.
27. K. Misawa, M. Tatsumoto, G. B. Dalrymple, K. Yanai, *Geochim. Cosmochim. Acta* **57**, 4687 (1993).
28. All samples were powdered in an aluminum oxide mortar and digested sequentially with concentrated HF, 8 N HNO_3, and 6 N HCl. Roughly 10% of the solution was split and spiked with ^{178}Hf and ^{186}W, whereas the remaining solution was dried and redissolved in ~8 ml of 4 N HF. The chemical separation of W was adopted from the first column of the Hf chemistry developed by Salters and Hart (*42*) but on a reduced scale with 3.5 ml of Bio-Rad AG1 ×8 (200 to 400 mesh) anion resin. The Hf and W were eluted and collected sequentially with the use of a mixed solution of 6 N HCl and 1 N HF. The same chemical procedure was used for the spiked solutions, but the column volume was further reduced (~1 ml) and Hf and W were collected together. Total procedural blank for W was ~0.4 ng. The multiple-collector inductively coupled–plasma mass spectrometry (MC-ICPMS) W isotopic measurement was the same as previously described (*43*), except for the use of a Cetac Technologies MCN6000 instead of the Mistral, a desolvating nebulizer. The NIST-3163 W standard was run in between every sample to monitor the performance of the MC-ICPMS and to check for memory effects, which were negligible. All W isotopic measurements were normalized to $^{186}W/^{184}W = 0.927633$ (*43*). The quoted 2σ standard errors all refer to the least significant figures. The isotope dilution measurements of Hf and W were determined simultaneously, and the reproducibility was typically 0.2% or better.
29. D.-C. Lee and A. N. Halliday, *Science* **274**, 1876 (1996).
30. ———, *Nature* **388**, 854 (1997).
31. $$\varepsilon_W = \left[\frac{(^{182}W/^{184}W)_{sample}}{(^{182}W/^{184}W)_{standard}} - 1\right] \times 10^4$$
32. H. St. C. O'Neill, *Geochim. Cosmochim. Acta* **55**, 1135 (1991).
33. G. J. Wasserburg and D. A. Papanastassiou, *Earth Planet. Sci. Lett.* **13**, 97 (1971); F. Tera, D. A. Papanastassiou, G. J. Wasserburg, *ibid.* **22**, 1 (1974); F. Tera and G. J. Wasserburg, *Proc. Lunar Planet. Sci. Conf.* **5**, 1571 (1974); D. A. Papanastassiou and G. J. Wasserburg, *ibid.* **6**, 1467 (1975); G. J. Wasserburg, D. A. Papanastassiou, F. Tera, J. C. Huneke, *Philos. Trans. R. Soc. London Ser. A* **285**, 7 (1977); E. C. Alexander, M. R. Coscio, J. C. Dragon, K. Saito, *Proc. Lunar Planet. Sci. Conf.* **11**, 1663 (1980); L. E. Nyquist and C.-Y. Shih, *Geochim. Cosmochim. Acta* **56**, 2213 (1992); C. Alibert, M. D. Norman, M. T. McCulloch, *ibid.* **58**, 2921 (1994).
34. F. J. Spera, *Geochim. Cosmochim. Acta* **56**, 2253 (1992).
35. A. N. Halliday *et al.*, *Earth Planet. Sci. Lett.* **133**, 379 (1995).
36. H. E. Newsom, W. M. White, K. P. Jochum, A. W. Hofmann, *ibid.* **80**, 299 (1986).
37. J.-L. Birck and C. J. Allègre, *ibid.* **124**, 139 (1994).
38. W. Yi, A. N. Halliday, D.-C. Lee, J. N. Christensen, *Geochim. Cosmochim. Acta* **59**, 5081 (1995).
39. The value of T_{CHUR} is defined as
$$T_{CHUR} = \frac{1}{\lambda} \ln\left\{\left(\frac{^{182}Hf}{^{180}Hf}\right)_{BSSI}\left[\frac{\left(\frac{^{180}Hf}{^{184}W}\right)_{sample} - \left(\frac{^{180}Hf}{^{184}W}\right)_{chond}}{\left(\frac{^{182}W}{^{184}W}\right)_{sample} - \left(\frac{^{182}W}{^{184}W}\right)_{chond}}\right]\right\}$$
where λ is the decay constant of ^{182}Hf (~0.077 m.y.$^{-1}$), $(^{182}Hf/^{180}Hf)_{BSSI}$ = bulk solar system initial isotopic composition = (2.4 ± 0.6) × 10^{-4} (*9*, *29*), and chond = chondritic. Model ages for samples with chondritic $^{182}W/^{184}W$ cannot be calculated.
40. P. H. Warren, *Am. Mineral.* **78**, 360 (1993).
41. O. B. James, M. M. Lindstrom, J. J. McGee, *Lunar Planet. Sci.* **XXI**, 603 (1991).
42. V. J. M. Salters and S. R. Hart, *Earth Planet. Sci. Lett.* **104**, 364 (1991).
43. D.-C. Lee and A. N. Halliday, *Int. J. Mass Spectrom. Ion Processes* **146/147**, 35 (1995).

44. We thank the Curation and Analysis Planning Team for Extraterrestrial Materials, NASA curatorial staff, and J. Gooding for supplying the Apollo lunar samples; H. Kojima, curator of the National Institute of Polar Research, Tokyo, for providing the lunar meteorite; and M. Garcia and C. Langmuir for supplying the terrestrial samples for this study. We thank J. N. Christensen, C. M. Hall, J. Jones, H. Palme, T. Pettke, M. Rehkämper, S. R. Taylor, and P. van Keken for comments; M. Johnson and Cetac Technologies for invaluable technical assistance; and R. M. Canup for a preprint. We acknowledge discussions with C. J. Allègre, A. G. W. Cameron, R. M. Canup, M. J. Drake, A. W. Hofmann, J. Jones, D. McKenzie, H. J. Melosh, R. K. O'Nions, D. A. Papanastassiou, D. Turcotte, G. J. Wasserburg, and B. J. Wood. This work was supported by the U.S. Department of Energy, NASA, NSF, and the University of Michigan.

1 August 1997; accepted 6 October 1997